Colloid Polym Sci (2005) 283: 653–661
DOI 10.1007/s00396-004-1197-x

ORIGINAL CONTRIBUTION

Hua Bao
George Chumanov
Richard Czerw
David L. Carroll
Stephen H. Foulger

Synthesis of core-shell silver colloidal particles by surface immobilization of an azo-initiator

Received: 31 December 2003
Accepted: 18 May 2004
Published online: 27 October 2004

D. L. Carroll · S. H. Foulger (✉)
School of Materials Science
and Engineering, Center for Optical
Materials Science and Engineering
Technologies, Clemson University,
Clemson, SC 29634, USA
E-mail: foulger@clemson.edu

H. Bao
School of Material Science
and Engineering, East China University
of Science and Technology,
Shanghai, 200237, P.R. China

G. Chumanov
Department of Chemistry,
Clemson University,
Clemson, SC 29634, USA

R. Czerw
Department of Physics and Astronomy,
Clemson University,
Clemson, SC 29634, USA

Abstract Silver nanoparticles, with the diameter of approximately 100 nm, were coated with a 5–10 nm layer of poly(styrene-*co*-4-styrene-sulfonic acid sodium salt). Polymerization was initiated on the particles by a surface adsorbed 4,4′-azobis(4-cyanovaleric acid) initiator. FTIR, electron microscopy, dynamic light scattering, and optical spectroscopy were employed to differentiate between the original and coated particles.

Introduction

The plasmon frequency of the conduction electrons in colloidal metal particles, particularly with diameters under 200 nm, results in unusual optical properties such as a strong optical resonance, large and fast nonlinear optical polarizability, and large enhancements in the local electric fields close to the metal surface [1]. Classical electromagnetic theory has been successful in describing these properties [2], which have led to a number of applications in, for example, optical filters [3], labeling in electron microscopy [4] and Raman spectroscopy enhancers [5].

Metal nanoparticles, particularly silver and gold, have been the focus of research not only because of their single particle optical properties, but also because of the prospect of using the collective response of metallodielectric colloids arranged in three-dimensional periodic arrays [6]. Unfortunately, metal particles tend to aggregate into disordered structures when manipulated

to particle densities in which crystallization into ordered arrays can occur. Coating an inorganic or organic layer around the metal particles enhances the ability to self-assemble the particles for further photonic applications, as well as the chemical resistance of the particles [7–14].

An approach to the preparation of a polymer layer attached to a substrate or particle is the use of immobilized initiators for the in situ generation of grafted polymers. Typically, modified azo compounds are used as surface initiators for the radical chain polymerization of vinyl monomers [15, 16]. In this article, we report on the coating of silver particles through the surface initiated free radical polymerization of a styrene copolymer. A carboxylic acid terminated azo-initiator, specifically 4,4′-azobis(4-cyanovaleric acid) (ACVA), was bound to the silver surface as carboxylate [17, 18] and then thermally decomposed to induce radical polymerization on the particle surface. A styrenesulfonic acid sodium salt was copolymerized with the styrene to increase the charge density of the coated particles and enhance their stability. FTIR, electron microscopy, dynamic light scattering (DLS), and optical spectroscopy were employed to differentiate between the original and coated particles.

Experimental section

Materials

Small silver colloidal particles were prepared by citrate and borohydrate reductions and are described elsewhere [19]. These particles were used as seeds to grow large particles by the same reduction reactions. Residual chemicals were removed by repeated centrifugation followed by redispersing in 18.2 MΩ cm water.

Styrene monomer was purchased from ACROS Organics (99.9%, ACROS). The monomer was washed with a 10% KOH water solution, and purified through reduced pressure distillation prior to use. In addition, 4-styrenesulfonic acid sodium salt hydrate (SSA-Na) (Aldrich Chemicals Company), poly(acrylic acid) (PAA) ($M_w \approx 2.5 \times 10^5$, 35 w/w solution in water, Aldrich Chemicals Company), and ACVA (97%, ACROS) were used as received.

Synthesis

In 2 ml of ethanol, 10 mg of the ACVA initiator was dissolved. This solution was then added to 8 ml of the silver colloid (particle density ca. 10^9–10^{10} cm^{-3}) and stirred for 4 h at room temperature. After stirring, 3.5 mg of PAA was added to the solution and the temperature of the system raised to 55 °C. Into this heated solution, 25 µl styrene and 25 µl of a 2% aqueous solution of SSA-Na were added at intervals of 15 min, for a combined total of 300 µl. The polymerization was then carried out for 16 h at 55 °C.

Particle characterization

The UV-Vis transmission spectra of the colloids were collected on an Ocean Optics PC2000 UV-Vis fiber optic spectrometer with incident light normal to the 1-cm pathlength quartz cuvette. Spectra were collected between the wavelengths of 300 and 800 nm.

Infrared spectra were recorded at a 4 cm^{-1} resolution on a Nicolet 560 FTIR spectrometer at a scan speed of 64 s^{-1}. The samples were prepared by spreading the coated silver colloids on a KRS-5 window and drying them under a heat lamp.

The diameters of the original and coated silver particles were measured with a Coulter N4 Plus DLS operating at a wavelength of 632.8 nm and at a temperature of 25 °C. Autocorrelation times were collected in excess of 600 s. The refractive index of bulk silver (i.e., $n = 0.56$ and $k = 4.27$) was used in the scattering normalization [20].

For electron microscopy imaging, both the silver colloids and the coated silver particles were dropped on Formvar carbon stabilized copper grids (Ted Pella Inc. 01753-FX1) and dried at room temperature under a watch glass. The samples were imaged using a Hitachi H-7000 transmission electron microscope (TEM) at an accelerating voltage of 100 kV and 20 μA, as well as a Hitachi HD-2000 scanning transmission electron microscope (STEM) at an accelerating voltage of 200 kV and 20 μA. Additionally, the silver particles were immobilized on poly(4-vinylpyridine) (PVP) coated glass [21] and then imaged on a Hitachi S-4700 scanning electron microscope (SEM) at an accelerating voltage of 5 kV. Image analysis was done with SigmaScan Pro Image Analysis V.5.0.

Results and discussion

FTIR spectroscopy

Figure 1 presents the procedure employed to coat the silver nanoparticles. Initially, the silver particles were mixed with ACVA for 4 h at room temperature in an effort to chelate the carboxylate group to silver surface sites [17, 22]. The propensity of silver nanoparticles to aggregate at elevated temperatures during polymerization motivated the incorporation of PAA as a steric stabilizer. It is speculated that the majority of the initiators are bound to the surface with one end. However,

after the initiator decomposes into its two halves, the second half may diffuse into the solution to initiate another polymerization reaction. Therefore, the coated colloids were centrifuged at 1,066 *g* for 30 min and washed with deionized water five times to separate the coated silver particles from pure polymer particles.

Though the silver nanoparticles have no discernable infrared signature, FTIR spectroscopy is useful to verify the presence of functional groups on the surface of the silver particles after the particles have been coated with a polymer. In Fig. 2a, the transmission FTIR spectra of the polystyrene-coated silver particles are presented after the completion of the emulsion polymerization and prior to any cleaning or separation procedure. In this spectrum, a number of vibrational bands characteristic of a carboxylic acid are present (e.g., 2,500–3,300 cm^{-1} for the O–H stretch, 1,720 cm^{-1} for the C = O stretch, C–O stretch twin peaks between 1,210 and 1,320 cm^{-1} , and the 1,395–1,440 cm^{-1} associated with the C–O–H bend) [23]. Both the ACVA initiator fragment and the PAA stabilizer could contribute this group to the spectra, though the absolute number of carboxylic acid groups contributed by the PAA exceeds the initiator fragment contribution, whereas in the original recipe, the ratio of carboxylic acid groups of PAA to ACVA was 3.4. In Fig. 2b, the particles were repeatedly washed with deionized water and centrifuged in an effort to remove any PAA in the solution. In this cleaned sample, the signature of carboxylic acid groups has been removed to a great extent, and the spectrum more closely resembles that of pure polystyrene (cf. Fig. 2c), with the characteristic absorbencies of a mono-substituted arene (e.g., the two or three bands between 3,000 and 3,070 cm^{-1} for the C–H stretch, the two or three bands between 1,500 and 1,600 cm^{-1} for the C = C stretch, the C = C–H out-of-plane bending at 730–770 and 680–720 cm^{-1}, and the two or three bands between 950 and 1,225 cm^{-1} attributed to ring torsion). In Fig. 2b, c, there are strong

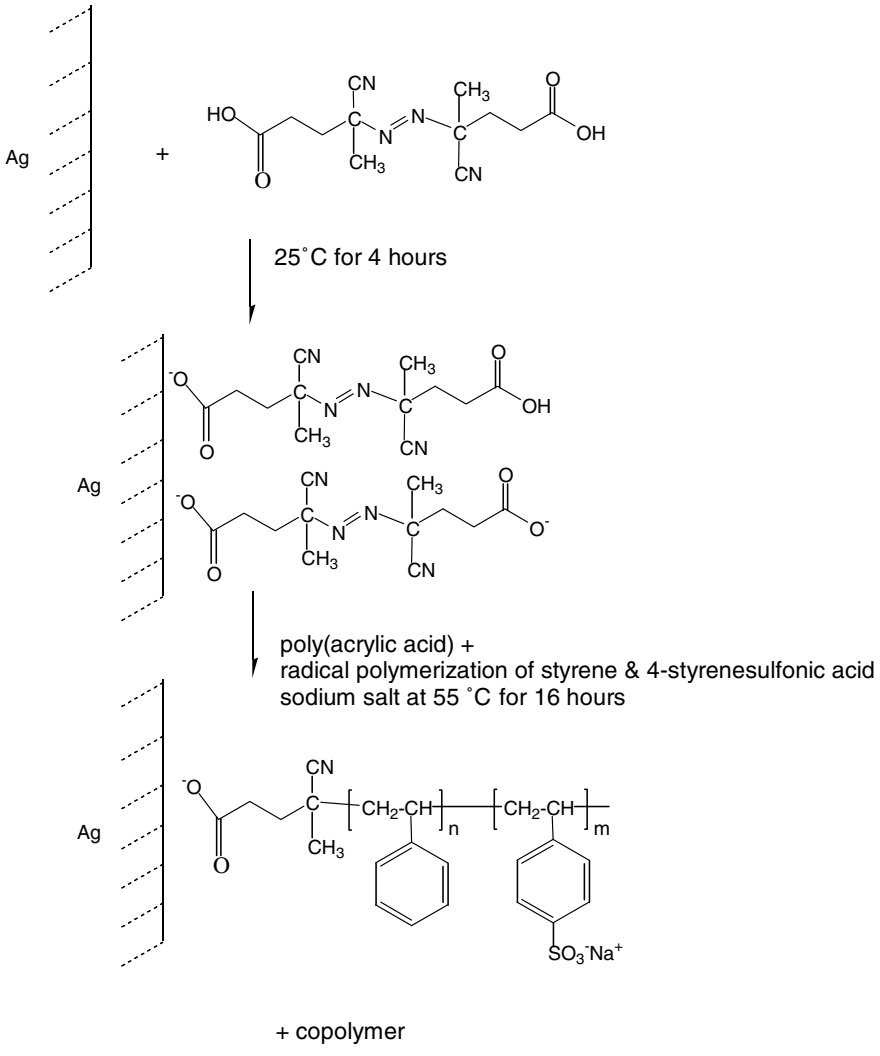

Fig. 1 Surface immobilization of an azo-initator on a silver particle and surface initiated radical polymerization

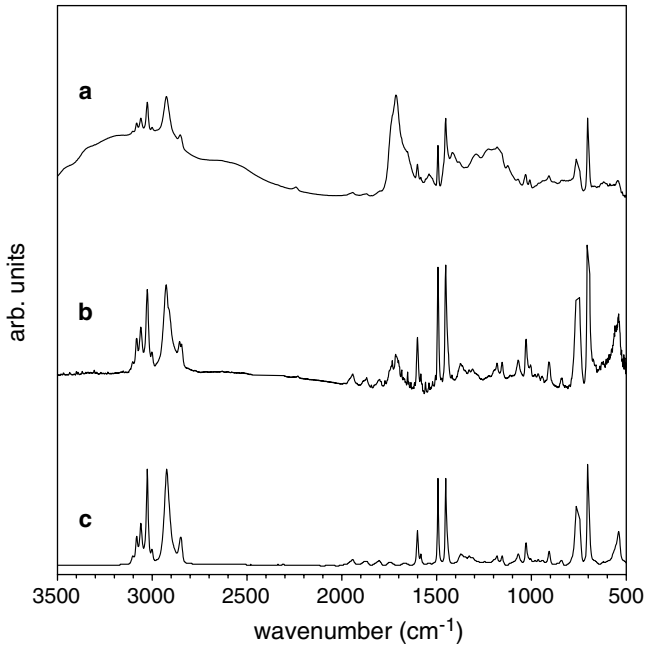

Fig. 2 Transmission FTIR spectra of **a** as produced by a coated silver colloid; **b** coated particles with repeated cleaning; **c** polystyrene standard; curves have been shifted for clarity

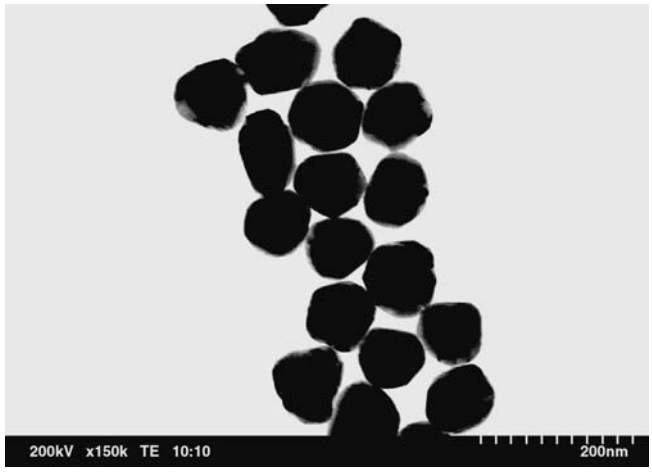

Fig. 3 BF-STEM micrograph of original silver colloidal particles

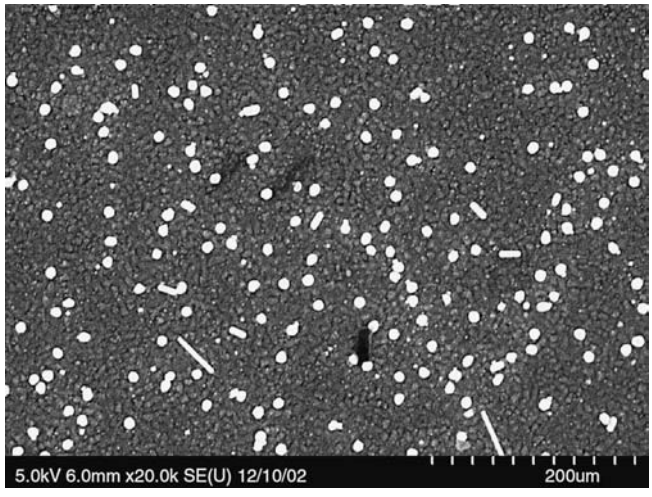

Fig. 4 Scanning electron micrograph of original colloidal silver particles immobilized on PVP [14]

absorbencies related to the alkane nature of the polymer with peaks between 2,850 and 3,000 cm^{-1} associated with the stretches of CH_3, CH_2, and CH. In addition, examining Fig. 2a closely, there appears to be a very small absorbence peak centered at 2,240 cm^{-1}, while in the cleaned sample (cf. Fig. 2b), this peak is reduced even further. This peak is attributed to the C–N stretch vibration and is assumed to be contributed by the initiator.

Electron microscopy

Although the infrared spectrum of the cleaned and coated silver colloids indicates the presence of a polystyrene coating, electron microscopy is a direct way to image the actual coating. In Fig. 3, the initial silver colloid is presented in a BF-STEM micrograph. By examining a number of different BF-STEM micrographs, and SEM images of the silver particles after they have been immobilized on a PVP-coated glass slide (cf. Fig. 4), it is possible to measure the dimensional characteristics of a large number of particles. From an analysis of a 200-member population, the silver particles appear to exhibit an elliptical shape in the two-dimensional analysis. Figure 5 presents the size distribution of the particles along its major axis (cf. Fig. 5a) and minor axis (cf. Fig. 5b), where the few ''rod-like'' silver particles that exhibited a major to minor axis ratio greater than three were not included. Figure 5 suggests a population of particles that are roughly 100 nm in diameter and accounts for ca. 82% of the particles, while there is a second, smaller population of particles that appear to be 40–50 nm in diameter and account for ca. 18% of the particles.

Dynamic light scattering (DLS) is useful in establishing the distribution of sizes in a solution of scattering particles. The refractive index of bulk silver (i.e., $n = 0.56$ and $k = 4.27$ at 633 nm [20]) was employed with Mie theory to convert the scattered intensities of the particles into a size and number distribution (cf. Fig. 6a). Silver particles greater than 20 nm exhibit only minor deviations in their dielectric properties relative to bulk silver [1]. The DLS analysis of the original colloid silver solution indicates a bimodal distribution of sizes, with one population of small ca. 20 nm diameter particles

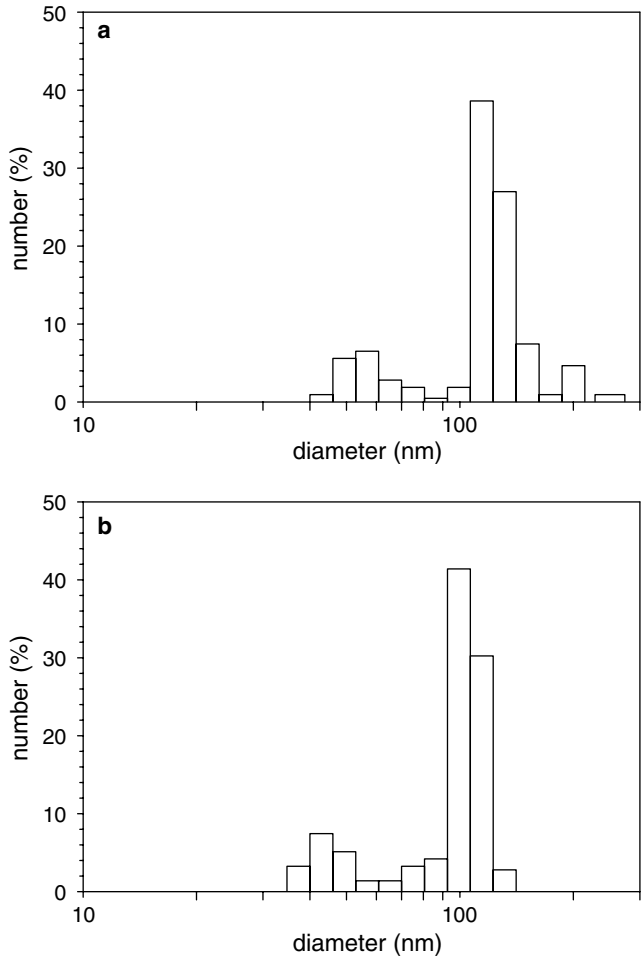

Fig. 5 Particle size as determined through image analysis of a scanning electron micrograph for original silver colloids along **a** major axis and **b** minor axis

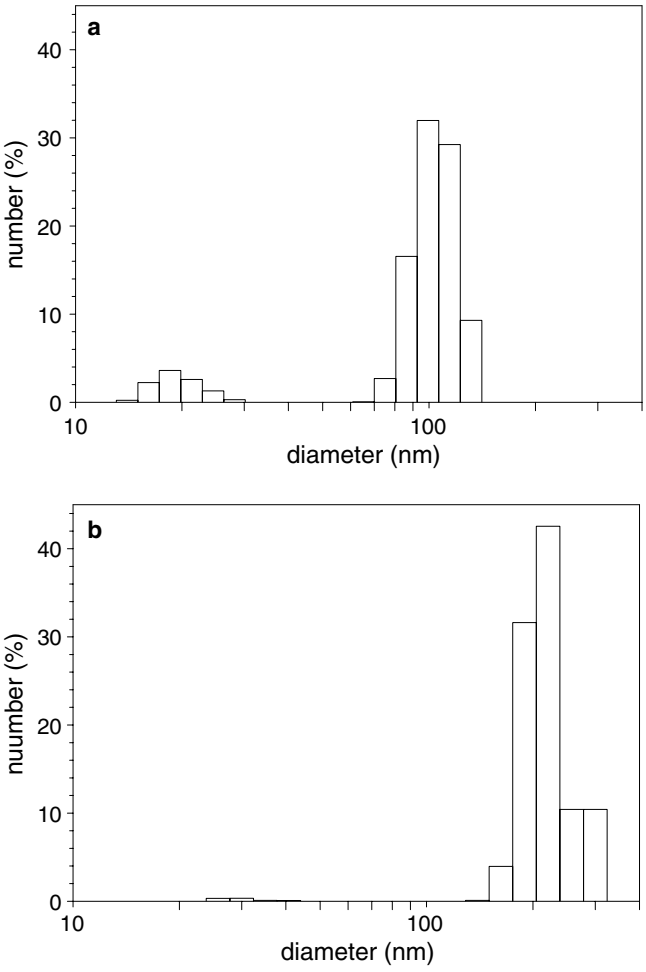

Fig. 6 Particle size as determined through DLS for **a** original silver colloids and **b** poly(styrene-*co*-4-styrenesulfonic acid sodium salt) coated silver particles. Refractive index of silver used $n = 0.56$ and $k = 4.27$; see Ref. [20]

and a second population centered around 104 nm which accounts for 93% of the total number of particles. Focusing only on this latter population of particles, the mean and standard deviation of this population is presented in Table 1. Since the DLS results are based on the hydrodynamic radius of an assumed diffusing sphere, there are bound to be discrepancies in assigning a single-dimensional parameter to particles which may not adhere closely to a spherical shape (cf. Fig. 3). Nonetheless, Table 1 indicates an agreement between these two approaches in determining the size of the larger distribution of particles within the first standard deviation of the population. The smaller population of silver particles observed in the DLS study is not apparent in the image analysis of the SEM micrographs. This latter technique may over-emphasize the population of larger particles through the sample preparation, where smaller particles may not be retained on the glass slide, as well as operator bias in the actual imaging.

Table 1 Particle diameter of silver colloids measured by scanning electron microscopy image analysis and DLS

	Original silver particles (nm)	Coated silver particles (nm)
SEM image analysis		
Long axis	118 ± 27[a]	–
Short axis	101 ± 25	
Dynamic light scattering[b] (DLS)	104 ± 16	194 ± 29

[a] 68% confidence values
[b] Refractive index of silver of $n = 0.56$ and $k = 4.27$ [20]

Figures 7 and 8 present TEM micrographs of the coated silver particles. The silver core has a higher electron density than the polymeric coating around the particle and therefore a metallodielectric core-shell structure is easily distinguished by TEM. In these

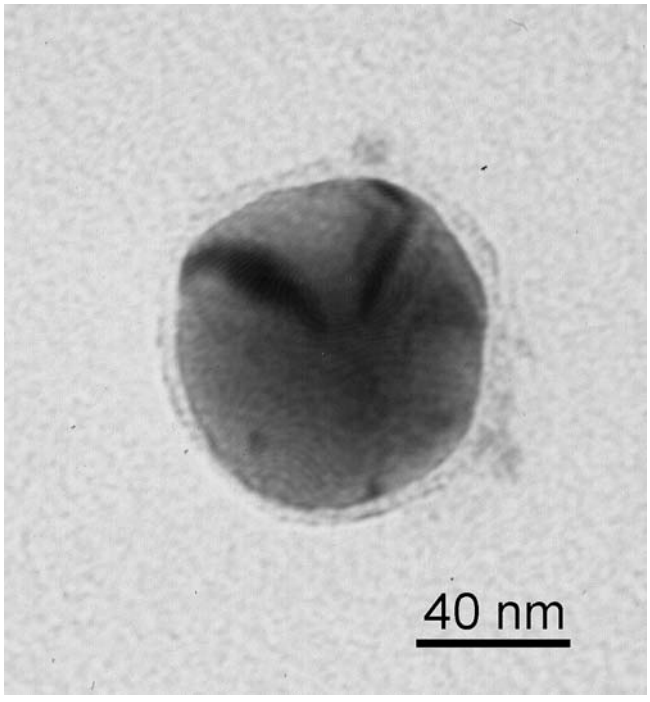

Fig. 7 TEM of a poly(styrene-*co*-4-styrenesulfonic acid sodium salt) coated single silver particle

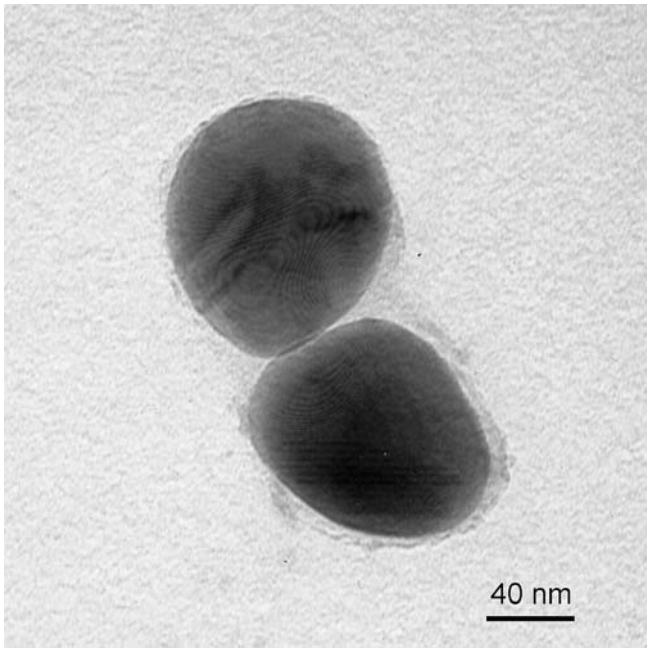

Fig. 8 TEM of a poly(styrene-*co*-4-styrenesulfonic acid sodium salt) coated duple silver aggregate

images, there is a clearly discernable ca. 5–10 nm coating of polymer on the outside of the particles. The corresponding DLS particle size distribution for these coated particles is presented in Fig. 6b. There appears to be a shift in the population of particles to larger diameters, as would be assumed with the coating of the particles. Based on Figs. 7 and 8, the ca. 104 nm diameter original silver particles would increase in diameter to a range of 120–130 nm after coating, but the distribution in Fig. 6b indicates a larger shift. Repeated STEM and TEM imaging of the coated particles indicates a large proportion of duple and triple aggregated particles (cf. Fig. 8). These aggregates would shift the population of particles out to greater diameters, increasing both the mean and standard deviation, relative to coated particles that were isolated. In addition, in Fig. 6b there appears to be a very small population of coated particles with a diameter of around ca. 30 nm, consistent with a 5–10 nm coating addition to the small particles centered at 20 nm of Fig. 6a.

Optical properties

It is informative to compare the predicted extinction efficiency of an isolated silver particle to the observed spectra of the original silver particles. Employing the DLS-derived diameter of the original silver particles, Fig. 9a presents the calculated extinction efficiency between the wavelengths of 300 and 800 nm of a silver particle, with a diameter of 104 nm, immersed in water [24], as well as the experimentally observed extinction spectra of the original silver particles. The observed spectra have been scaled relative to the calculated maximum. The total extinction efficiency is a combination of scattering and absorption, where the absorption of light by a metal particle has a physical origin in the coherent oscillation of the conduction band electrons induced by the electromagnetic field [1]. This surface plasma resonance of small metallic particles is determined by the density of electrons, the effective electron mass, and the shape and size of the charge distribution about the particle [25]. For simple geometries such as a small sphere, a single plasma resonance can be excited, while less symmetric or larger geometries can result in higher order multipole resonances. The calculated spectrum exhibits a maximum at 402 nm, attributed to a quadrupole resonance, and a global maximum at 502 nm, attributed to a dipolar resonance.

The experimentally observed spectrum for the original particles displays two broad maxima, one located at ca. 403 nm and a larger maximum at ca. 477 (cf. Fig. 9a). There is a reasonable agreement between the calculated and observed wavelength position of the quadrupole resonance, though the experimentally observed peak is less pronounced relative to the calculated resonance. This may be a consequence of the oblate shape of the particles, where the quadrupole mode has been shown to be ''quenched'' by particle asymmetry

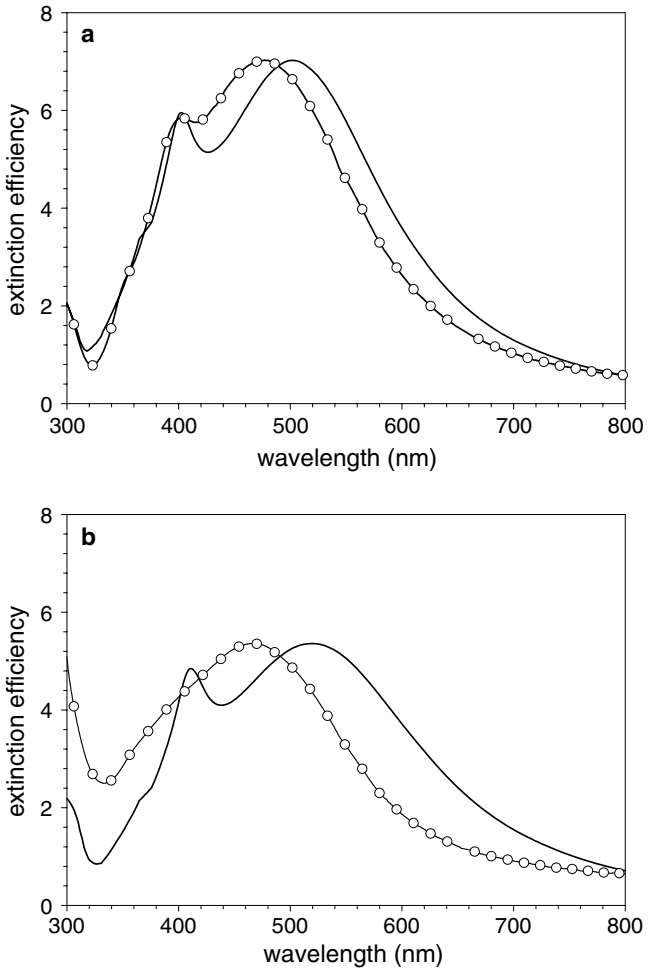

Fig. 9 **a** Calculated extinction efficiency of a 104-nm diameter silver sphere immersed in water (*solid line*) and the experimentally observed spectra of the original silver particles (*open circle*). **b** Calculated extinction efficiency of a 104-nm diameter silver sphere coated with a 10-nm polystyrene layer ($n = 1.6$) and immersed in water (*solid line*) and the experimentally observed spectra of the coated silver particles (*open circle*). The calculations are based on the implementation of Mie's theory as presented in Ref. [24] and employed the refractive index of silver of Ref. [26]. The experimentally observed spectra have been scaled relative to the corresponding calculated maximum

[27]. The observed dipolar resonance is ca. 25 nm red-shifted relative to the calculated position. This latter contribution to the extinction spectrum is significantly sensitive to the size and shape of the particles and the actual particles do not adhere to the unimodal characteristics of the hypothetical spheres employed in the calculations (cf. Table 1). In addition, both the experimentally observed and calculated spectra exhibit a sharp minimum at ca. 320 nm, corresponding to a minimum in the imaginary part of the refractive index [20].

Figure 9b presents the calculated extinction efficiency of a silver particle immersed in water, with a diameter of 104 nm and coated by a 10 nm layer of polystyrene [24], as well as the experimentally observed extinction spectra of the coated silver particles. Though the two calculated spectra of a coated and uncoated particle (cf. Fig. 9a) are similar in appearance, there is a bathochromic shift of 16 nm for the dipolar resonance with the inclusion of the polymer coating. According to the Mie theory, the position of the extinction peak of an isolated metallic particle is predicted to appear at longer wavelengths as the refractive index of the continuous medium increases, a prediction often borne out in experiments [28]. In the experimentally observed systems, the refractive index of the continuous medium of the original particles is water, while the coated particles are encased in a polymeric layer with a larger refractive index of ca. 1.6. The expectation is that the coated particles would exhibit a bathochromic shift of the dipolar resonance, though the peak is observed to exhibit a hypsochromic shift of ca. 12 nm (peak position at 465 nm) relative to the original particles. The maximum in the extinction spectrum is sensitive to a change in the refractive index of the continuous medium as well as the state of particle aggregation. Metal particles can undergo two forms of aggregation which leads to distinct differences in the observed optical spectra. One form of aggregation leads to the electron overlap of the clustered particles and results in a "single" electrically conducting entity that exhibits a red-shift of the observed plasmon resonance relative to the isolated particles. In the second form of aggregation, the particles cluster but are electrically isolated from one another by an insulating layer. These latter clusters will exhibit a blue-shift of the observed plasmon resonance relative to the isolated particles. In the present case, the thin polymer coating on the particles is speculated to electrically insulate the particles from one another. If the coated particles exhibit irreversible aggregation resulting in chained clusters, it is possible that the system could exhibit a hyposchromic shift [1, 29]. This aggregation is consistent with both the DLS and TEM analyses (cf. Fig. 8 and Table 1) of the coated particles, which suggest a moderate level of aggregation of the particles after they were coated.

An additional investigation on the nature of the coating on the silver particles was conducted through the addition of nitric acid to the original and coated particles. Figure 10a presents the change in the extinction spectrum of the uncoated colloid with various nitric acid exposure times. The uncoated silver particles can react with nitric acid forming a soluble nitrate salt that does not exhibit the peaked extinction spectrum of the metallic particles. The nitric acid quickly reduces the number and size of the silver particles, as evidenced by the reduction in extinction efficiency and the shift in the dipolar resonance contribution of the original extinction spectrum to shorter wavelengths (cf. Fig. 11), respectively.

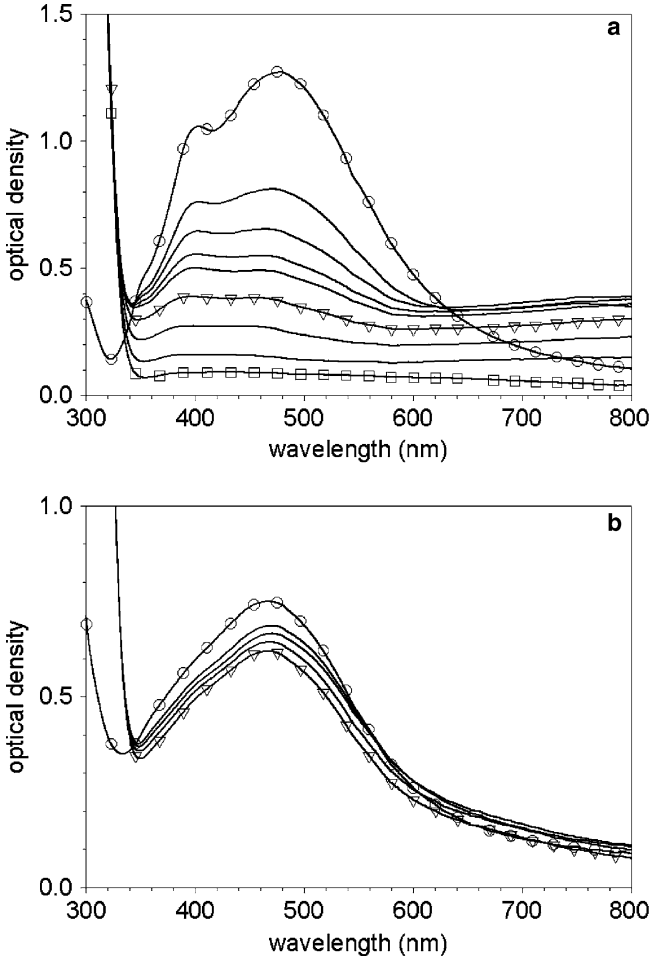

Fig. 10 Optical density of **a** a silver colloid mixed with nitric acid at 0 (*open circle*), 25, 50, 100, 200, 800 (*open inverted triangle*), 1,600, 3,000, and 5,000 (*open square*) and **b** a coated silver colloid mixed with nitric acid at various exposure times: 0 (*open circle*), 25, 400, 1,200, 2,000, 4,000, and 6,000 (*open inverted triangle*) seconds

After the encapsulation of the silver particles, the polymer layer surrounding the particles significantly reduces the diffusion of the nitric acid into the silver cores, as evidenced by Fig. 10b. There appears to be an initial drop in the extinction maximum and then a slow change in the peak maximum with time. It is speculated that the initial drop is due to the dissolution of uncoated particles that have not been removed in the centrifugation process, and particles that do not have complete coverage. The particle density of the coated silver particles was lower than in the original silver suspension, as evidenced by the lower extinction values. By insuring that the ratio of nitric acid to colloid solution was maintained at the same level between the two samples

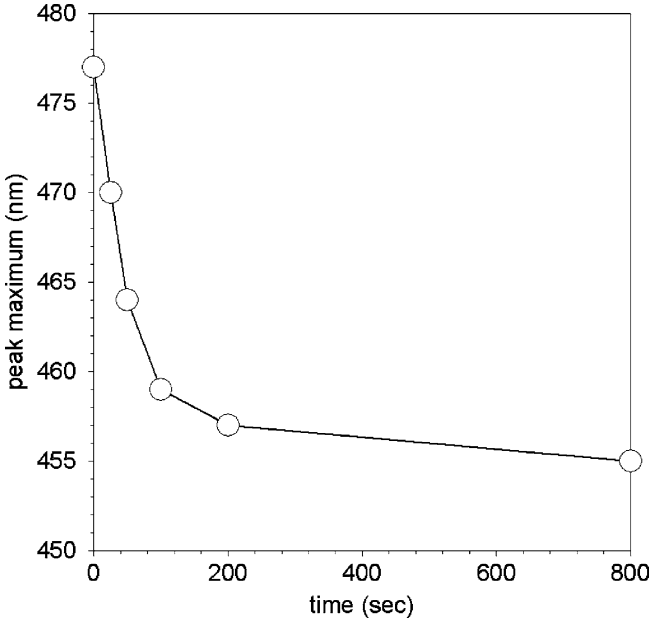

Fig. 11 Position of dipolar extinction maximum of a silver colloid mixed with nitric acid at various exposure times

employed (Fig. 10), the resulting silver-to-nitric acid ratio of the coated particles would be higher relative to the original silver suspension and would also be a severe test on the ability of the coatings to prevent the access of the acid to the cores.

Conclusion

Silver nanoparticles, with the diameter of approximately 100 nm, were coated with a 5–10 nm layer of poly(styrene-*co*-4-styrenesulfonic acid sodium salt). Polymerization was initiated on the particles by a surface adsorbed ACVA initiator. FTIR, electron microscopy, and DLS were employed to characterize the original and coated particles. By monitoring the optical properties of the silver particles, the resistance to nitric acid of the particles with a polymeric coating was confirmed. Minor changes in the extinction spectrum of the coated particles were observed with lengthy exposures to nitric acid, while the original silver particles exhibited major changes with comparable exposure times.

Acknowledgements The authors would like to thank DARPA (Grant Number: N66001-01-1-8938) for financial support, while one author (S.F.) would specifically like to thank the 3M Corporation for a Non-Tenured Faculty Award and the National Science Foundation for a CAREER award (DMR-0236692).

References

1. Kreibig U, Vollmer M (1995) Optical properties of metal clusters. Springer, Berlin Heidelberg New York
2. Mie G (1908) Ann Phys 25:377
3. Dirix Y, Bastiaansen C, Caseri W, Smith PC (1999) Adv Mater 11:223
4. Bendayan M (2000) Histochem 75:203
5. Nie SR, Emroy SR (1997) Science 275:1102
6. Zhou J, Zhou Y, Ng SL, Zhang HX, Que WX, Lam YL, Chan YC (2000) Appl Phys Lett 76:3337
7. Gittins DI, Caruso F (2001) J Phys Chem B 105:6846
8. Graf C, van Blaaderen A (2002) Langmuir 18:524
9. Jordan R, West N, Ulman A, Chou YM, Nuyken O (2001) Macromolecules 34:1606
10. Liz-Marzan LM, Mulvaney P (2003) J Phys Chem B 107:7312
11. Mandal TK, Fleming MS, Walt DR (2002) Nanolett 2:3
12. Obare SO, Jana NR, Murphy CJ (2001) Nanolett 1:601
13. Ohno K, Koh K, Tsujii Y, Fukuda T (2002) Macromolecules 35:8989
14. Quaroni L, Chumanov G (1999) J Am Chem Soc 121:10642
15. Prucker O, Ruhe J (1998) Macromolecules 31:602
16. Schmidt R, Zhao T, Green JB, Dyer DJ (2002) Langmuir 18:1281
17. Moskovits M, Suh JS (1985) J Am Chem Soc 107:6826
18. Smith EL, Porter MD (1993) J Phys Chem 97:8032
19. Chumanov G, Sokolov K, Gregory B, Cotton TM (1995) J Phys Chem 99:9466
20. Johnson PB, Christy RW (1972) Phys Rev B 6:4370
21. Malynych S, Luzinov I, Chumanov G (2002) J Phys Chem B 106:1280
22. Wang W, Chen X, Efrima S (1999) J Phys Chem 103:7238
23. Szymanski H (1964) IR: theory and practice of infrared spectroscopy. Plenum Press, New York
24. Bohren CF, Huffman DR (1983) Absorption and scattering of light by small particles. Wiley, New York
25. Kelly KL, Coronado E, Zhao LL, Schatz GC (2003) J Phys Chem B 107:668
26. Palik ED (1985) Handbook of the optical constants of solids. Academi, San Diego, p 351
27. Kottmann JP, Martin OF, Smith DR, Schultz S (2001) Phy Rev B 64:235402
28. Zeiri L, Efrima S (1992) J Phys Chem 96:5908
29. Kerker M (1985)J Colloid Interface Sci 105:297